

# COMSOL Modelling of a Planar Micro Ion Mobility Spectrometer

R. Cumeras<sup>1\*</sup>, I. Gràcia<sup>1</sup>, E. Figueras<sup>1</sup>, L. Fonseca<sup>1</sup>, J. Santander<sup>1</sup>, M. Salleras<sup>1</sup>, C. Calaza<sup>1</sup>, N. Sabaté<sup>1</sup>, C. Cané<sup>1</sup>

<sup>1</sup>Instituto de Microelectrónica de Barcelona. IMB-CNM (CSIC). Campus UAB, 08193 Bellaterra (Barcelona) Spain.

\*Corresponding author: ph.: +34-935947700, fax: +34-935801496, e-mail: raquel.cumeras@imb-cnm.csic.es

**Abstract:** A micro Planar Ion Mobility Spectrometer (P-FAIMS) has been simulated using FEM Multiphysics software. In P-FAIMS target ions are discriminated by the application of the proper separation voltages to the electrodes of the system. Modelling of vapour phase ions of two compounds have been studied for different values of electric field amplitude to gas number density ( $E/N$ ) ratio: a health risky volatile acetone  $\text{Ac}_2\text{H}^+$  ion, and a chemical warfare agent simulant  $\text{DMMPH}^+$  ion that emulates gas sarin. Results shows that simulations of ions behaviour in a P-FAIMS are possible with COMSOL Multiphysics software and that the time and intensity at which ions are detected are in good agreement with experimental data found in the literature.

**Keywords:** P-FAIMS; Ion Mobility Spectrometer; FEM Gas Simulation.

## 1. Introduction

Ion Mobility Spectrometry (IMS) is an analytical technique based on ion separation in gaseous phase due to an electric field. It has fundamental advantages such as high resolution ( $\sim$ ppb) and fast measurements ( $\sim$ ms). IMS devices have a typical minimum volume about  $40\text{cm}^3$ , but due to the trend towards miniaturization of ion mobility spectrometers, smaller volumes ( $\sim$ mm<sup>3</sup>) are being explored [1-3]. IMS shows good separation capability for multiple ions with short response time, and especially  $\mu$ IMS's allow low temperature operation with higher sensitivity compared to other IMS implementations [2]. All these advantages make IMS a rapidly advancing technique with a wide spectrum of applications, including detection of chemical warfare agents and explosives [4].

In this work the modelling, with COMSOL Multiphysics software, of a micro planar Ion Mobility Spectrometer (P-FAIMS) is presented with the aim of detect and discriminate between  $\text{DMMPH}^+$  and  $\text{Ac}_2\text{H}^+$  ions, as representative

examples of possible cohabitation of various vapours in security applications.

In presence of an electric field, ions with different collision cross-sections temporally separate based on the frequency of ion-neutral interactions. Continual micro-scale acceleration and scattering collisions deceleration of ions results in a constant average velocity, the drift velocity  $v_d$  (m/s); that is directly proportional to the magnitude of the applied electric field strength  $E$  (V/cm) [5]:

$$v_d = K \cdot E \quad (1)$$

where  $K$  (cm<sup>2</sup>/Vs) is the ion mobility coefficient, characteristic of each ion and each medium, and is the basis for its identification.

## 2. P-FAIMS working principle

The implementation of a strong time-dependent electric field as a periodic asymmetric waveform in P-FAIMS electrodes, perpendicular to ions displacement is used to separate and select them (shown in Figure 1). This is allowed taking advantage of the slightly dependence of the ion mobility with strong fields. Using an adequate AC  $E$  field the ions are displaced of their main path depending of their mobility dependence to the  $E$  field, and only one type can reach the detector [1-3].

The mobility of a given ion at constant temperature and pressure with gas density  $N$  (m<sup>-3</sup>) through a drift gas under the influence of a high electric field can be expressed by [6]:

$$\begin{aligned} K(E/N) &= K_0(1 + \alpha(E/N)) \\ &= K_0 \left[ 1 + \alpha_2 \cdot (E/N)^2 + \alpha_4 \cdot (E/N)^4 + \dots \right] \end{aligned} \quad (2)$$

where  $K_0 = K(E/N)_{E=0}$  is the ion mobility at low electric field for an specific medium number density  $N$  (m<sup>-3</sup>); and  $\alpha(E/N)$  describes ion mobility dependence on the electric field at a constant density of drift gas at atmospheric

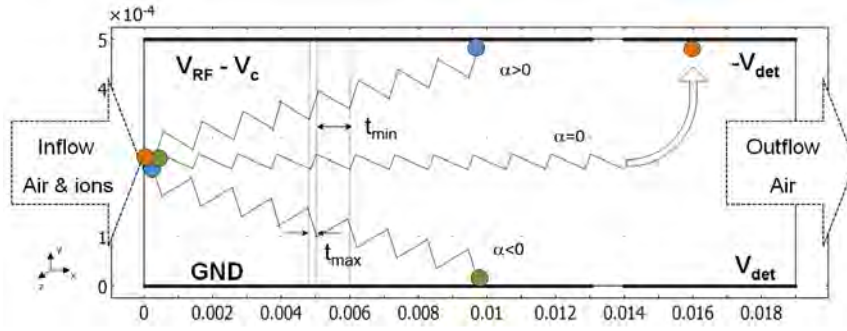


**Figure 1.** Schematic of the P-FAIMS drift channel defined by filtering and detector electrodes. Ion paths are schematized under the influence of RF and DC fields for the filtering region and the detector fields for detection region.

pressure and constant temperature.  $E/N$  is the electric field in Townsend ( $1 \text{ Td} = 10^{-17} \text{ Vcm}^2$ ) units. Equation (2) is a convenient mathematical expression for the alpha function [7].  $K_0$ ,  $\alpha_2$ , and  $\alpha_4$ , are characteristic of each ion and are obtained experimentally. When electric field exceeds  $10000 \text{ V/cm}$  ( $E/N \sim 40 \text{ Td}$ ) the mobility of some ions varies.

As can be seen in Figure 1, one of the plates is grounded and the other is biased at high voltage with an asymmetric waveform,  $V_{RF}(t)$ , satisfying that its integration over a period has to be zero. While all ions interact with the applied RF field and are drawn towards the drift channel walls, selected ions can be kept in the flowing gas by applying particular low DC voltage or compensation voltage ( $V_C$ ) that prevents the ion migration towards either electrode. Thus, a selected ion passes through the filter electrodes and reaches the detector being this  $V_C$  voltage a characteristic of each ion species.

### 3. 2D Modelling Planar-FAIMS

COMSOL Multiphysics software is used to simulate the behaviour of two different vapour ions in a P-FAIMS. The software takes into account nonlinear combined effects of different forces and concentrations fields. Created model combines fluid dynamics and electric field which have been found to be the most significant effects. Other effects such as electric repulsion in ion cloud due to space charge have been found to be considerably less significant [8] (for the low concentration level simulated, 1ppm) and thus were not included in the simulations presented.

Model assumptions are resumed in Figure 2. Drift gas velocity in the P-FAIMS gap has been calculated using the Navier-Stokes module.

Electric potentials applied to the filtering and detector electrodes are calculated using the conductive media DC module and, ions behaviour under their influences is calculated with electrokinetic flow module.

A 2D approximation as shown in Figure 1 is done considering that all the effects do not vary along the electrodes width for the two electrode regions defined: 1) filtering electrodes, of  $13 \times 5 \text{ mm}^2$  separated by  $0.5 \text{ mm}$  gap, where the AC and DC voltages needed to filter the different ionic species are defined 2) detector electrodes of  $5 \times 5 \text{ mm}^2$  placed  $1 \text{ mm}$  after filtering electrodes to collect ions and generate the  $V_C$  spectrum. Drift gas ( $\text{N}_2$ ) enters through all the channel height from the left and ions enter the channel through a narrow space  $\Delta z = 0.02 \text{ mm}$  at the center of the gap, passes through the filtering area and only 'selected' ions reach the detector electrodes.

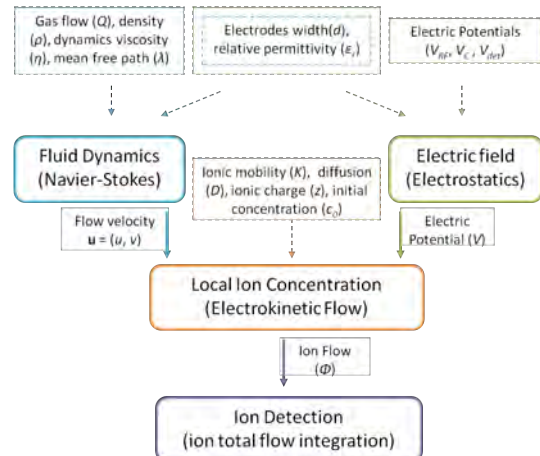


**Figure 2.** Block diagram of key computational steps involved in modelling P-FAIMS with COMSOL software. Straight squares indicate main modules and dashed squares indicate variables needed for the modules.

### 3.1 Fluid Dynamics

Drift gas (N<sub>2</sub>) flow modelling is determined by the incompressible Navier-Stokes equations:

$$\rho \frac{\partial \mathbf{u}}{\partial t} - \nabla \cdot \eta (\nabla \mathbf{u} + (\nabla \mathbf{u})^T) + \rho \mathbf{u} \cdot \nabla \mathbf{u} + \nabla p = \mathbf{F} \quad (3)$$

where  $\rho$  is the fluid density,  $\mathbf{u}$  is the velocity vector,  $\eta$  is the dynamic viscosity,  $T$  is the temperature,  $p$  is the pressure and  $\mathbf{F}$  is the term of forces actuating on the body.

Gas flows in pipes or between parallel plates in laminar or turbulent regime determined by the dimensionless Reynolds number. In our case, for an inlet gas flow of  $Q=1$  l/min, Reynolds number obtained is  $Re \sim 400$ , this value is 10 times lower than the turbulence onset threshold ( $Re \sim 4000$ ), so the gas flow is considered to be laminar.

Drift gas simulations have been operated at a temperature of 298K and a pressure of 760Torr, being the number density of nitrogen  $N = 2.5 \times 10^{25} \text{ m}^{-3}$ . It is also considered that the pressure of drift gas and the ions is the same, so nitrogen does not vary its pressure as it is confined between two parallel plates and because sample enters for the centre of the gap and has no expansion due to pressure.

In Figure 4 the modelled velocity of nitrogen in the drift channel is shown for the graphic of the x-velocity of nitrogen for an arbitrary x-scale. It can be seen the laminar behaviour of the drift gas when flows at  $Q = 1$  l/min, with a maximum x-velocity of 10 m/s.

### 3.2 Electric Fields:

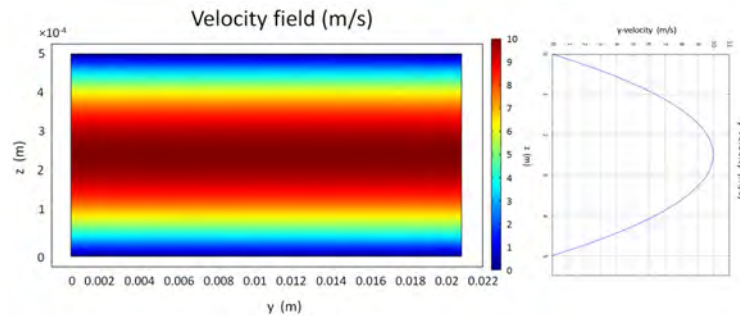


**Figure 3.** Velocity field of nitrogen at the drift channel obtained with Navier-Stokes module for an inlet gas flow of  $Q = 1$  l/min, showing the laminar behaviour of  $y$ -velocity of N<sub>2</sub> in an arbitrary  $y$ .

Detector electrodes have been biased at  $\pm 5V$  and total electric voltage applied at the filtering electrodes has been defined as:  $V_T = V_{RF} - V_C$ . Applied separation voltage  $V_{RF}$  is defined as [9]:

$$V_{RF}(t) = V_{RF} \cdot [2 \sin(\omega t) + \sin(2\omega t - \pi/2)]/3 \quad (4)$$

where for all simulations, the frequency of the waveform applied has been set to  $\nu_{RF} = 2\text{MHz}$  [1-2, 5],  $V_{RF}$  is shown in Figure 3. It is needed to achieve a compromise between frequency and gap. A low frequency implies that the positive high-voltage  $V_{max}$  is applied for a longer time and ions will travel a longer distance toward the filtering electrodes and eventually they will be lost before reaching the detector.

### 3.3 Ion Concentration:

Flow of charged ions subject to an electric field verifies the mass conservation law defined from Nernst-Planck equation that takes into account diffusion, convection and migration flows:

$$\nabla \cdot (-D\nabla c + \mathbf{u}c - z_{ion}Kc\nabla V) = R = 0 \quad (5)$$

where  $c$  is ion concentration (mol/m<sup>3</sup>),  $D$  is ion diffusion (m<sup>2</sup>/s),  $z_{ion}$  is ions charge number (adim),  $K$  is ion mobility coefficient (cm<sup>2</sup>/V·s),  $V$  is the voltage affecting the ion (V),  $R$  is reaction rate (mol/(m<sup>3</sup>·s)) that is supposed to be zero -Ions do not interact with one another- and  $\mathbf{u}$  is the air velocity (m/s) affecting ion species. Modelled ions concentrations have been fixed to 1 ppm in all studied cases.

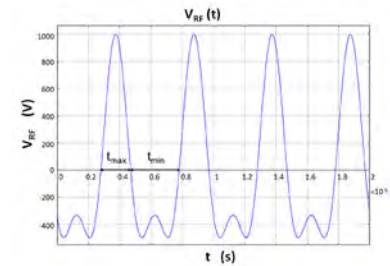


**Figure 4.** Separation voltage as applied to the modelled P-FAIMS.

**Table 1:** Parameters used in simulations for the studied compounds [9-10].

Chemical	Ion Acronym	$K_0$ ( $10^{-4}$ m <sup>2</sup> /V·s)	$\alpha_2$ (Td <sup>-2</sup> )	$\alpha_4$ (Td <sup>-4</sup> )
2-propanone (Ac)	Ac <sub>2</sub> H <sup>+</sup>	1.88 [9]	$1.34 \cdot 10^{-5}$	$1.77 \cdot 10^{-9}$
Dimethyl methylphosphonate (DMMP)	DMMPH <sup>+</sup>	1.94 [10]	$5.09 \cdot 10^{-6}$	$-1.58 \cdot 10^{-10}$

### 3.4 Ion Detection:

The local concentration of ions within the drift region and its dependence from the parameters above mentioned allows computing the ion current at the collector. Integrating the normal component of ions flux per unit area  $A$  (mm<sup>2</sup>) of the collector with normal vector  $\mathbf{n}$  yields the ion current [18]:

$$I = \int_A \mathbf{n} F z_{ion} \Theta_{EK} dA = \int_{x,z} \mathbf{n} F z_{ion} \Theta_{EK} dx dz \stackrel{2D \text{ approx}}{=} d \int_x F z_{ion} \Theta_{EK} dx \quad (6)$$

where  $F$  (= 96.485C/mol) is the Faraday constant [19]. As considering 2D simulations we are assuming that  $z$ -intensity is uniform for the whole detectors width. This integral has been defined by 'integration coupling variables' option from the COMSOL software, before performing the simulations.

### 3.5 Simulation simplifications

Modelled ions are analyzed once inside the P-FAIMS, and non-ionized molecules form part of the drift gas. To simplify numerical simulations, following assumptions are accepted during the time the ions travel through the device: 1) All ions are singly charged 2) Ions are assumed to be free from clusters -from water vapour and nitrogen in the ionization process- 3) Ions do not interact with one another, so that interactions resulting from space charging do not occur 4) Ions do not have dipolar moment 5) Ions do not react within themselves or other molecules. These assumptions are contained, in part, for the experimental parameters and it would be redundant to take them into account again.

### 3.6 Experimental data

The absolute mobility scale enabling comparisons between IMS data at different  $N$  is established by introducing the reduced mobility:

$$K_0 = K \frac{P T_0}{P_0 T} = K \frac{N}{N_0} \quad (7)$$

where the mobility is normalized to pressure  $P$  and temperature  $T$  for the value for standard conditions for temperature and pressure (STP):  $T_0 = 298\text{K}$  and  $P_0 = 760\text{Torr}$ ; or to the gas number density (the number of molecules per unit volume), for the value of the Loschmidt constant:  $N_0 = 2.687 \times 10^{25} \text{ m}^{-3}$ .

Simulations have been done with experimental data available at the literature [9-10], and the main properties needed or:  $K_0$ ,  $\alpha_2$  and  $\alpha_4$ , are summarized in Table 1.

## 4. Results and Discussion

For low RF electric fields ( $E/N < 40$  Td) there is no dependence of mobility with electric field, therefore  $V_C = 0$  V for all ions. Increasing electric field they can be separated due to their differences on mobility coefficients. Ions with the same rate  $E/N$  also have the same  $V_C$ .

In Figure 5, the results for the simulated compounds in  $N_2$  are showed. For  $E/N < 40\text{Td}$ , is not possible to differentiate the ions and all are detected at the same time. For  $40\text{Td} < E/N < 78\text{Td}$  ions can be differentiated but intensity current peaks are overlapped. For  $E/N = 73\text{Td}$  Ac<sub>2</sub>H<sup>+</sup> and DMMPH<sup>+</sup> compensation field value is equal. And for  $E/N > 78\text{Td}$  ions are fully differentiated.

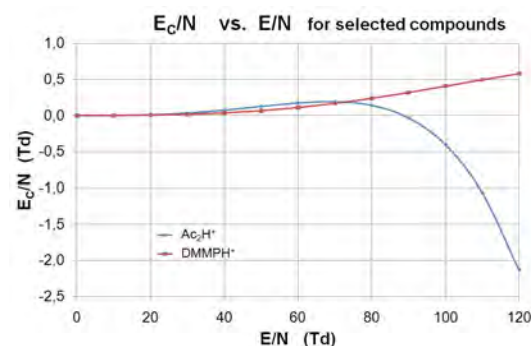


**Figure 5.** Obtained compensation fields for simulated compounds.



As can be seen in Figure 5,  $\text{Ac}_2\text{H}^+$  and  $\text{DMMPH}^+$  ions behaviour is different because they have different  $\alpha_2$  and  $\alpha_4$  values (the parameters that define the mobility of the ion). In fact, the  $\text{DMMPH}^+$  is a type A ion ( $\alpha$  increases as  $E/N$  increases) while  $\text{Ac}_2\text{H}^+$  is a type B ion ( $\alpha$  initially increases as  $E/N$  increases and then decreases with further increase in  $E/N$  after reaching a maximum).

In Figure 6 is shown the distribution of the ions concentration through the drift channel for  $\text{Ac}_2\text{H}^+$  and  $\text{DMMPH}^+$  and for two different separation voltages.  $\text{DMMPH}^+$  ion concentration is shown as line contour plots whereas  $\text{Ac}_2\text{H}^+$  ion concentration is drawn by a continuous surface plot. Concentrations of Acetone and DMMP ions are presented for two different situations: A) for  $V_{RF} = 875\text{V}$  ( $E_{RF}/N = 73\text{Td}$ ): Acetone and

$\text{DMMPH}^+$  ions reach the detector for the same value of  $V_C = -2.3\text{V}$  ( $E_C/N = 0.19\text{Td}$ ) showing that for just certain values of the applied voltage ion with the same DC voltages will not be separated. B) for  $V_{RF}=1000\text{V}$  ( $E_{RF}/N = 79\text{Td}$ ) shows good discrimination for a  $V_C = -1.9\text{V}$  ( $E_C/N=0.15\text{Td}$ ) detecting only  $\text{Ac}_2\text{H}^+$ : the  $V_C$  that allows the detection of each component is well differentiated at these electric fields.

Results obtained from simulations showed that ion discrimination could be achieved with COMSOL software and that it is a good platform for this kind of simulations. Obtained intensities for initial concentrations of 1ppm, are in all cases of the order of nA.

## 5. Conclusions and Prospect

Simulations of a P-FAIMS have been done with COMSOL Multiphysics software for Acetone and DMMP compounds in vapour phase. Discrimination of these compounds has been studied for a value range of  $E/N$  from 0 to 120 Td, showing that for  $E/N < 40\text{Td}$ , is not possible to differentiate the ions, in good agreement with experimental data. From  $E/N \geq 40$  Td it is possible to differentiate  $\text{DMMPH}^+$  from  $\text{Ac}_2\text{H}^+$ , but for  $40\text{Td} < E/N < 78\text{Td}$  intensity current peaks are overlapped, being for  $E/N > 78\text{Td}$  fully differentiated.

From the encouraging simulation results, the fabrication of the P-FAIMS instrument device will be addressed using micro-electro-mechanical systems fabrication techniques.

## 6. References

1. R.A. Miller, G.A. Eiceman, E.G. Nazarov, A.T. King, A novel micromachined high-field asymmetric waveform-ion mobility spectrometer, *Sensors and Actuators B: Chemical* 67 300-306 (2000).
2. R. Guevremont, R.W. Purves, Atmospheric pressure ion focusing in a high-field asymmetric waveform ion mobility spectrometer, *Rev. Sci. Instrum.* 70 1370-1383 (1999).
3. M. Salleras, A. Kalms, A. Krenkow, M. Kessler, J. Goebel, G. Muller, S. Marco, Electrostatic shutter design for a miniaturized ion mobility spectrometer, *Sensors and Actuators B: Chemical* 118 338-342 (2006).

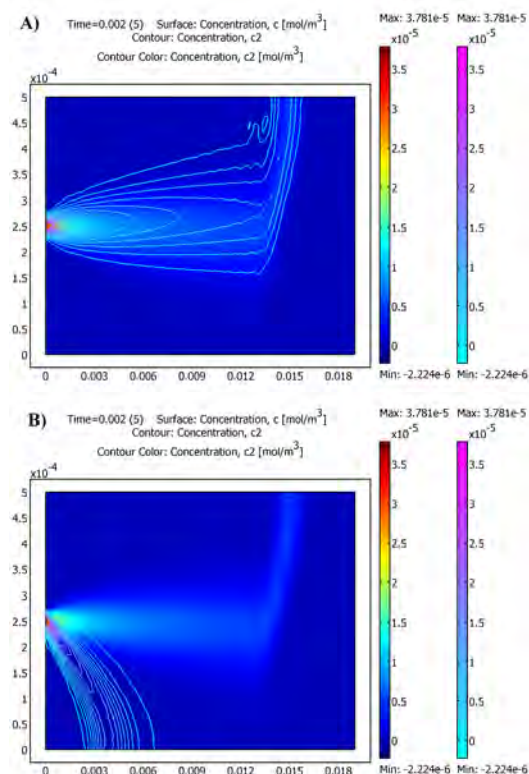


**Figure 6.** Simulation concentrations of  $\text{Ac}_2\text{H}^+$  ion -represented by continuous surface plot- mixed with  $\text{DMMPH}^+$  ion -represented by line contour plots-. For a separation voltage of A)  $V_{RF} = 875\text{V}$  ( $E/N = 73\text{Td}$ ), both ions have the same  $V_C = -2.3\text{V}$  ( $E_C/N = 0.19\text{Td}$ ) and are attracted to the same detector electrode. No differentiation is obtained. B)  $V_{RF}=1000\text{V}$  ( $E/N = 79$  Td), and for a  $V_C = -1.9\text{V}$  ( $E_C/N = 0.15\text{Td}$ ) only  $\text{Ac}_2\text{H}^+$  detection is obtained. Differentiation is achieved.

4. B.M. Kolakowski, Z. Mester, Review of applications of high-field asymmetric waveform ion mobility spectrometry (FAIMS) and differential mobility spectrometry (DMS), *Analyst* 132 842-864 (2007).
5. G.A. Eiceman, Z. Karpas, *Ion Mobility Spectrometry*. CRC Press, Boca Raton (1993).
6. A.A. Shvartsburg, *Differential Ion Mobility Spectrometry: Nonlinear Ion Transport and Fundamentals of FAIMS*. CRC Press, Boca Raton, FL (2009).
7. E.V. Krylov, E.G. Nazarov, R.A. Miller, Differential mobility spectrometer: Model of operation, *Int. J. Mass Spectrom.* 266 76-85 (2007).
8. D.A. Dahl, T.R. McJunkin, J.R. Scott, Comparison of ion trajectories in vacuum and viscous environments using SIMION: Insights for instrument design, *Int. J. Mass Spectrom.* 266 156-165 (2007).
9. E. Krylov, E.G. Nazarov, R.A. Miller, B. Tadjikov, G.A. Eiceman, Field dependence of mobilities for gas-phase-protonated monomers and proton-bound dimers of ketones by planar field asymmetric waveform ion mobility spectrometer (PFAIMS), *J. Phys. Chem. A* 106 5437-5444 (2002).
10. N. Krylova, E. Krylov, G.A. Eiceman, J.A. Stone, Effect of moisture on the field dependence of mobility for gas-phase ions of organophosphorus compounds at atmospheric pressure with field asymmetric ion mobility spectrometry, *J. Phys. Chem. A* 107 3648-3654 (2003).

## 7. Acknowledgements

This work and PhD Thesis grant of Ms. R. Cumeras have been financially supported by the Spanish Ministry of Science and Innovation MICINN-TEC2007-67962-C04-01 project.